Indian Journal of Chemical Technology
Vol. 31, September 2024, pp. 738-748
DOI: 10.56042/ijct.v31i5.9238

Sequestration of Ni(II) ions from water bodies by using gamma-sterilized biowaste

Apurva Bambal[1], Ravin Jugade[1]*, D. Sarvanan[2] & Yogesh Pakade[3]

[1]Department of chemistry, RTM Nagpur University, Nagpur 440033, India

[2]Department of Chemistry, National College, Tiruchirappalli, Tamilnadu-620001, India

[3]Cleaner Technology and Modeling Division, CSIR-NEERI, Nagpur-440010, India

*E-mail: ravinj2001@yahoo.co.in

Received 02 March 2024; accepted 22 August 2024

Nickel has been recognized as an essential element in proper growth and development of plants and has wide range of physiological and morphological functions. But high concentrations of Nickel affect to the metabolic activity of plants. Therefore, it is essential to remove Ni(II) from water bodies. Cow-dung (CD) has been reported to be an adsorbent due to nitrogen containing functional groups that are capable of complexing various metal ions. The purpose of this work was to adsorb Ni(II) from an aqueous solution using CD. The bacterial contamination associated with CD has been overcome by sterilizing it by gamma irradiation dose of 4 kGy forming γ-CD. FTIR, SEM-EDX, XRD, and TGA-DTA techniques are used to characterize γ-CD. At solution pH of 5.0, adsorption capacity of is found to be 23.88 mg/g demonstrating monolayer adsorption. Equilibrium kinetics for adsorption is explained by pseudo-secondorder model. Intraparticle diffusion model was studied to know that diffusion is not a rate limiting step. The thermodynamic parameters like ΔG, ΔS and ΔH are computed by van't Hoff equation. The negative values of ΔG and ΔH specifies spontaneity as well as exothermic behavior of the adsorption process. Column studies are also performed to check its applicability for larger volumes of sample.

Keywords: Adsorption, Cow dung, Gamma sterilization, γ-CD, Kinetics, Thermodynamics

Introduction

These days, anthropogenic heavy metal pollution of wastewater is an issue that needs to be resolved. Various heavy metals such as chromium, nickel, cadmium are considered as very toxic pollutants. Their toxicity can cause multiple organ damage even at low concentrations[1]. Various techniques such as chemical precipitation[2], ion exchange[3], reverse osmosis[4] and electro-floatation[5] were used for removal of these toxic pollutants, but all these techniques have some drawbacks like production of toxic sludge, high energy and low efficacy. Biosorption is interesting process because of its low cost and high efficacy[6].

Any material which is contaminated with the biological substances refers as biowastes. Various biowaste materials are present in nature such as waste dried activated sludge biomass[7], natural sugarcane bagasse[8] and brewery sludge[9] but cow dung (CD) has ample amount of lignin, cellulose and hemicellulose. There are different minerals like nitrogen as well as phosphorus with some trace elements like sulphur, iron, magnesium, cobalt, copper etc[10]. One of such metal is Ni(II)[11]. On one hand, Ni(II) has been recognized as a vital element for numerous important biological processes like strong growth of plants, animals, and soil microbes, while excess amount uplifts flora and fauna[12]. According to the guidelines given by WHO, the maximum allowable concentration of Ni(II) ions in drinking water should be 0.02 ppm[13]. Hence from aqueous bodies, it is compulsory to confiscate Ni(II).

CD has been proven to be the cheapest and easily available biosorbent in nature[14]. CD has been reported to be adsorbent due to nitrogen containing functional groups that are capable of complexing various metal ions as well as dyes[15]. However, its application as an adsorbent could not be exploited due to a large concentration of micro-organisms present in it. In order to overcome this problem of microbial contamination associated with this excellent adsorbent, this paper reports sterilization of cow dung by irradiation with gamma radiations leading to sterilization. After gamma sterilization, the number of bacterial count present in the CD was tremendously decreased as we increase the gamma dose making the material suitable for nickel removal from aqueous media.

Experimental Section

Loba Chemical Pvt. Ltd., Mumbai, India supplied Nickel sulphate pentahydrate, Dimethyl glyoxime (DMG), liquid bromine and liquor ammonia. Whatmann filter paper no. 1 was purchased from Hi-Media Pvt. Ltd. For all reagents preparations, Millipore water (conductivity <1 µs) was used.

From a nearby cow shade, CD cake was obtained. It was dried under sunlight for 7 days. After complete drying, the CD cake was crushed finely. This crushed CD was washed many times with hot double distilled water until it lost its original smell, color and led to neutral pH. Lastly, the material was oven dried at 50°C. The dried CD was run through 500 µm diameter sieve. The finely powdered CD was gamma sterilized under various doses. The results obtained shows that the microbial count was tremendously decreased at 4 kGy dose. The γ-CD was stored in airtight container and used as per requirement.

Gamma sterilization of CD was carried out by using GC-1200 (BRIT, India), an indigenous source of gamma radiation operating at 4.219 kGy h^{-1} dose rate. Thermal stability of γ-CD was analyzed by using DTG-60 simultaneous TG / DTA equipment (Shimazdu) in nitrogen medium. Bruker-Alpha-spectrometer was employed to record FTIR spectrain range from 500-4000 cm^{-1}. From FT-IR spectra the functional and structural aspects of γ-CD could be described. X-ray diffractometer instrument make Righaku-Minifex 300 was used to record X-ray diffractogram. Surface characteristic properties were scanned using TESCAN VEGA 3 SBH. For elemental analysis, Oxford INCA Energy 250 EDS system was employed based on EDX spectrum. pH meter from Equiptronics with model number EQ-615 was employed to adjust pH of the solution. For uniform mixing of solutions, mechanical shaker REMI RS-12R DX (REMI, India) was used.

Batch adsorption trials were conducted to assess the adsorption efficiency. At pH 5, 25 mL of 100 mg L^{-1} adsorbate solution was used. 100 mg γ-CD was equilibrated and stirred for contact time of 60 min. After 60 min of adsorption period, by using filter paper (Whatmann filter paper no. 1), supernatant liquid was filtered. From supernatant, 1 mL adsorbed Ni(II) solution was taken into volumetric flask of 25mL. Later 1 mL liquor ammonia and 1 mL bromine water were added and made up the volume with double distilled water up to the mark. The Ni(II) estimation was carried out by using dimethylglyoxime reagent spectrophotometrically. Maximum adsorption efficiency was projected by using following formula given below.

$$q_e = \frac{(Co-Ce)V}{W} \quad \ldots (1)$$

Percent removal was determined as follows.

$$\% \text{ Removal} = \frac{(Co-Ce)}{Co} \times 100 \quad \ldots . (2)$$

Results and Discussion

Characterization of γ-CD

To ascertain the thermal stabilities of materials along with their compositional qualities, TGA and DTA measurements are largely utilized. Change in a mass shows degradation of material. The sample illustrates reduction in weight into three stages as shown in (Fig. 1a). The initial weight loss up to 100°C assures loss of moisture. Remarkable and rapid weight loss was shown from temperature range of 250°C and 400°C which was the next deprivation step. The second degradation approximately 48% shows the pyrolysis was primarily responsible for losses of organic materials like cellulose and hemicellulose. The third degradation found in between 350°C-900°C which shows 25.97% weight loss. This decrease can be explained by thermal decomposition of aromatic compounds, including lignin and some extractives. The total weight loss from was found to be 86.84%. The DTG curve's trend is in line while TGA curve has been shown in (Fig. 1b). The moisture loss is accompanied by endothermic peak while thermal degradation of γ-CD was accompanied by exothermic peak in DTA curve[16].

FTIR spectrum (Fig. 1c) of γ-CD provides clear indication of presence of functional groups. There are various peaks present in FTIR spectrum of CD corresponding to the existence of various adsorptive functional groups, which confirms functionality of γ-CD as an adsorbent (Fig. 1c). O-H stretching, N-H stretching and C-H stretching vibrations were represented by the peaks at 3225 cm^{-1}, 3450 cm^{-1} and 2900 cm^{-1}, respectively[17]. Stretching of C=O is indicated by the noticeable double peak at 1725 cm^{-1}. N-H bending causes the significant peak at 1650 cm^{-1}, C-N stretching causes the peak at 1180 cm^{-1}.

X-ray diffractogram of γ-CD (Fig. 1d) shows substantial amount of cellulose, which contributes the existence of peaks between 17° and 23°. However, the

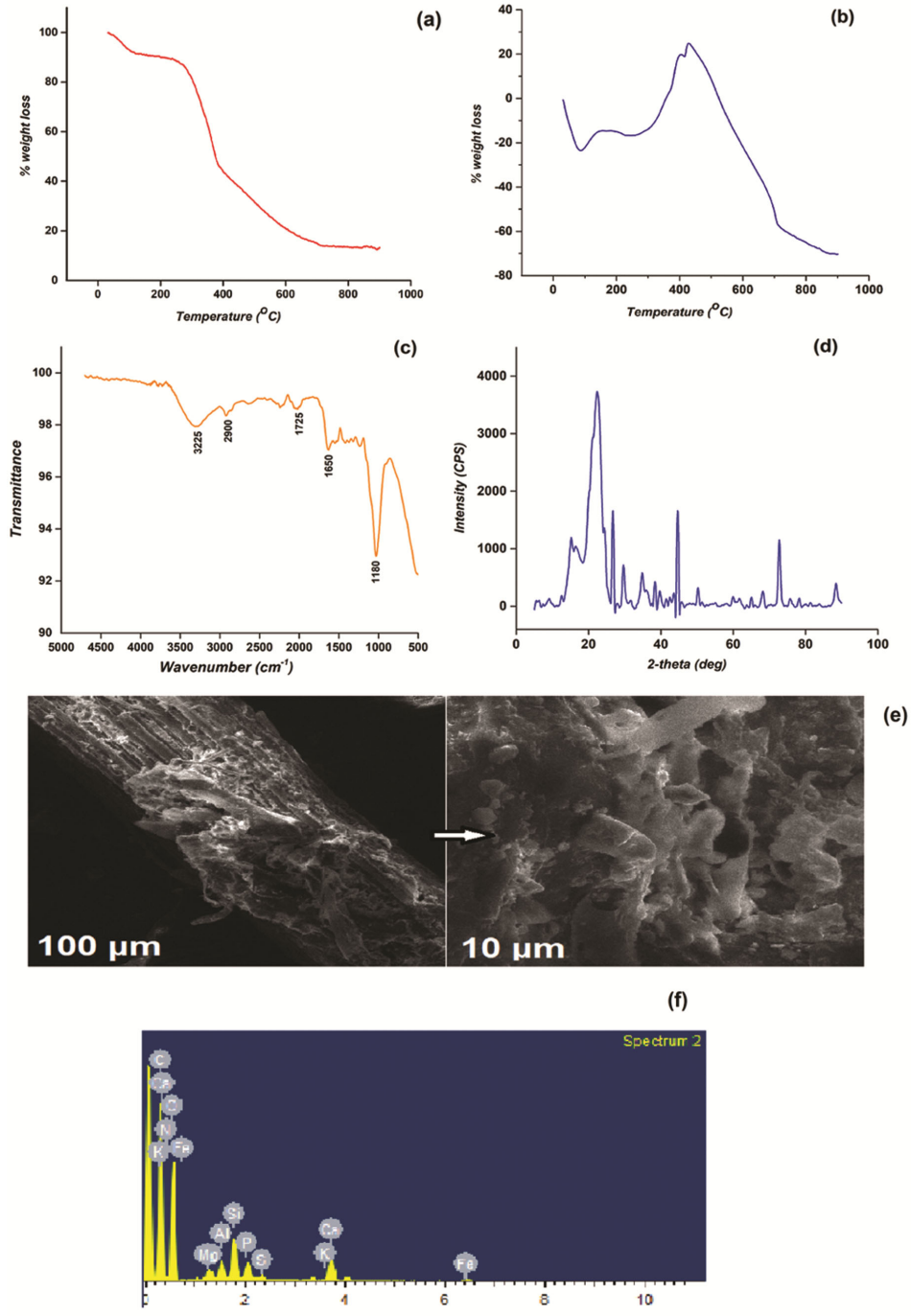

Fig. 1 — (a) TGA curve (b) DTA curve (c) FTIR spectrum (d) XRD plot (e) SEM images at different resolutions (f) EDX spectrum of γ-CD

complex nature of this biomaterial can be revealed from the complex XRD pattern[10].

Relative proportions and elemental contributions in γ-CD have been illustrated with the help of EDX spectrum (Fig. 1d). The primary C and Ca peaks can be seen along with other elemental peaks such as N, O, Si, Mg, Al, P, S, K[18].

Lignin and cellulose are the main and primary components of CD. SEM images validate fibrous structure of γ-CD. The surface of γ-CD was found to be rough, dense and porous containing rod-like granules which are linked by tissues having a threadlike appearance. γ-CD has many micro, macro and tiny apertures which ensures high surface area[19].

Gamma sterilization of cow-dung

CD is mainly embracing lignin, cellulose and fibrous materials[2]. There are ample of minerals and minimal amounts of sulphur, iron, magnesium, copper, cobalt as well as manganese. However, the usage of CD in water treatment is not recommended due to microbial contamination associated with it. In order to overcome this problem, the CD was irradiated with gamma radiations from ^{60}Co source[20]. Various gamma doses ranging from 1 kGy to 8 kGy were given to 2.0 g CD samples taken in zip bags. From each sample, 0.1 g of CD was re-suspended in 9 mL of saline water and then onto nutrient agar plate 0.1 mL of sample was spread. The nutrient agar plates were diluted 1000 times. The sample was incubated for 48 h. The number of colonies in agar plates were calculated as per g of sample taken. Fig. 2 shows decrease in microbial activity with increase in gamma dose. The bacterial count was found to be negligible above gamma dose of 4 kGy and above. So, 4 kGy dose was selected as optimum dose for further studies. The CD sterilized by giving this dose has been nominated as γ-CD and used in all adsorption experiments.

Batch adsorption experiments

Effect on pH

Study of pH effect is the key factor to assess the adsorption efficiency of an adsorbent from aqueous medium. pH dependency of metal adsorption is related to ionic state of functional groups which are present on adsorbent[21]. They strongly affect surface charge as well as degree of utilization.

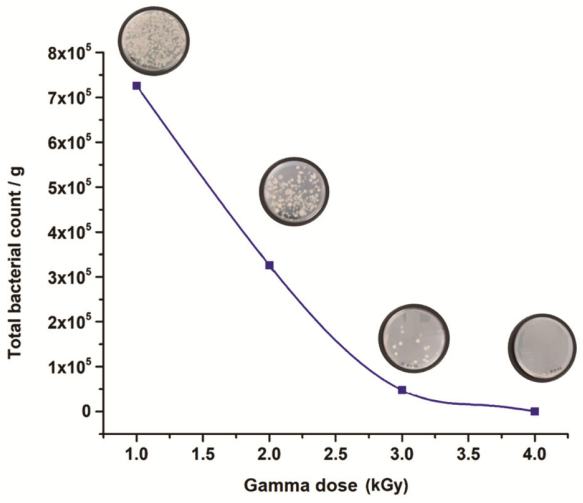

Fig. 2 — Sterilization of cow-dung by gamma irradiation

The initial concentration of Ni(II) was subjected to pH alteration from 2.0 to 9.0 utilizing dilute solutions of 0.1 M sodium hydroxide (NaOH) and 0.1 M hydrochloric acid (HCl). 100 mg of γ-CD adsorbent was added to 25 mL of adsorbate solutions followed by 60 min of stirring. The results shown in Fig. 3a depicted that Ni(II) ions elimination did not significantly alter over entire pH range. At pH 5.0, the percentage removal was about 76.25%. Hence. pH 5.0 was taken into consideration for rest studies.

Effect on dose

Effect on adsorbent dose is the key parameter to observe smallest quantity that demonstrates the maximum adsorption[22]. Dose was varied from 25 to 500 mg for 60 min. It was detected that with the increase of adsorbent dose, the adsorption efficiency also increases and finally it reaches to the saturation point at 100 mg dose (Fig. 3b). Hence, 100 mg dose was designated for future studies.

Effect on contact time

To study the impact of contact time, fixed amount of γ-CD at specific concentration of each solution, the exposure duration for which the adsorbent is in contact with the adsorbate was changed between 5 min to 120 min. The findings shows that adsorption effectiveness increased as contact duration rose to 60 min with equilibrium adsorption capacity (Fig. 3c).

Effect on concentration

Initial concentration has a substantial impact on the adsorption process which effectively push the molecule of solute against the obstacle to mass transfer between the solid and liquid phase[23]. To study the concentration effect, various concentrations of Ni(II) were varied from 25-500 mg L^{-1} for all the solutions in order to explore influence of early concentrations of adsorbate at optimal pH, contact time, and adsorbent dose on removal capability of adsorbent. Hence for further studies, 100 mg L^{-1} concentration was selected. (Fig. 3d).

Adsorption isotherms

To model the adsorption studies, Langmuir and Freundlich isotherm models were employed for better understanding of the interactions between the adsorbate and adsorbents[10]. For better adsorbent selectivity and performance of an adsorption system, adsorption isotherms were used[24]. By equilibrating 25 mL of different concentrations ranging from 25 to

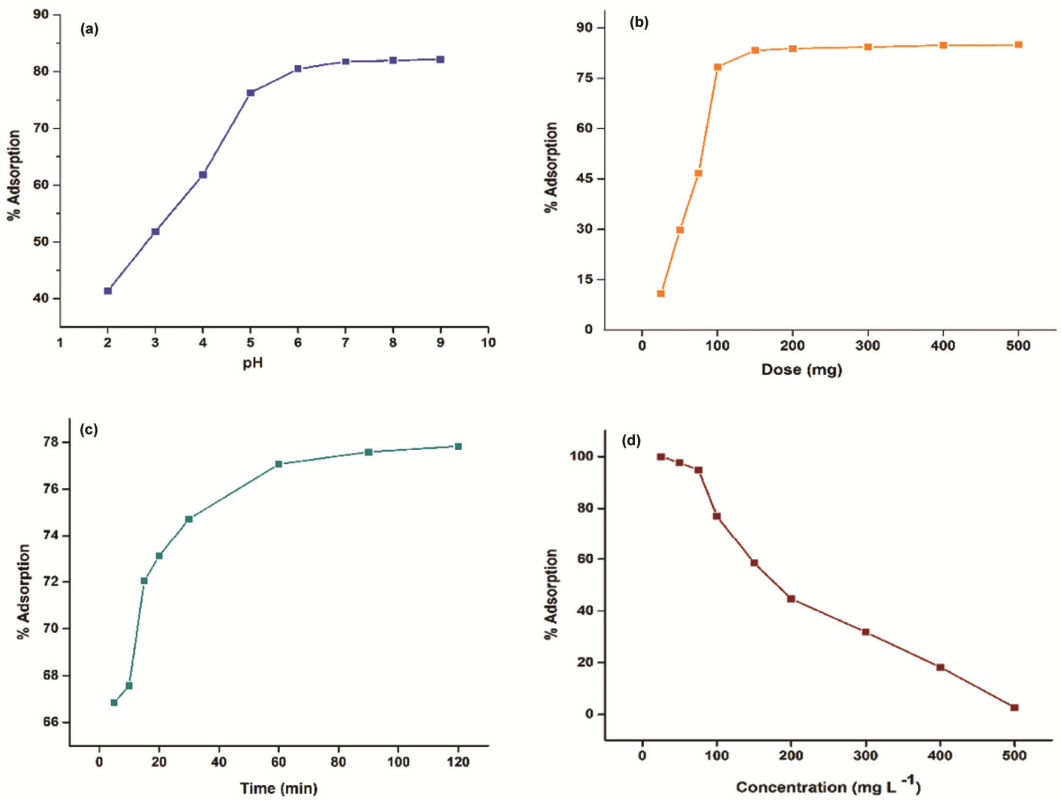

Fig. 3 — Effect of (a) initial solution pH (b) adsorbent dose (c) adsorption time (d) initial concentration of Ni(II) ions (general conditions: pH = 5, adsorbent dose = 100 mg, adsorption time = 60 min, concentration = 100 mg L^{-1})

500 mg L^{-1} keeping pH 5.0 with dose of 100 mg for period 60 min, the data were measured. If there is monolayer adsorption on the homogeneous surface of adsorbent, then Langmuir isotherm model fits well. In this case there is negligible lateral interactions[25]. The linear and non-linear forms of Langmuir isotherm model are stated in Eqs (3) and (4), respectively.

$$\frac{C_e}{q_e} = \frac{1}{q_m \times K_L} + \frac{C_e}{q_m} \quad \ldots (3)$$

$$\mathbf{q_e} = \frac{\mathbf{q_{max} \times K_L \times C_e}}{\mathbf{1 + K_L \times C_e}} \quad \ldots (4)$$

The maximum adsorption capacity q_{max} (mg/g) was found from the slope as well as intercept of the plot of C_e against q_e. Adsorption capacity (q_e) of 23.88 mg g^{-1} shows adsorption behaviour of adsorbent towards Ni(II). Figs 4 (a) and (b) illustrate linear and non-linear plots for Langmuir model.

Freundlich isotherm model is used to study simultaneous solute adsorption on non-uniform surfaces which explains exponential distribution with adsorption energy[21]. The linear as well as non-linear forms of Freundlich adsorption model are expressed in Eqs (5) and (6), respectively.

$$\log q_e = \log K_f + \frac{1}{n} log C_e \quad \ldots (5)$$

$$\mathbf{q_e} = \mathbf{K_F} \times \mathbf{C_e^{1/n}} \quad \ldots (6)$$

Where K_F denotes efficiency of adsorption and n shows the intensity of adsorption. The values of K_F (mg g^{-1}/ng L^{-1}) and non-linear graph was attained from slope as well as intercept of the plot between q_e versus C_e respectively. Figs 4 (c) and (d) show linear and non-linear plots, respectively, for Freundlich model.

From the values of regression coefficients (Table 1) and the plot of experimental q_e values of both the isotherms against C_e, the Langmuir adsorption isotherm model emerged as best fit model. This shows monolayer adsorption of Ni (II) on γ-CD surface.

Kinetics of adsorption

Adsorption kinetics is one of the most vital parameters to study and evaluate the time dependency

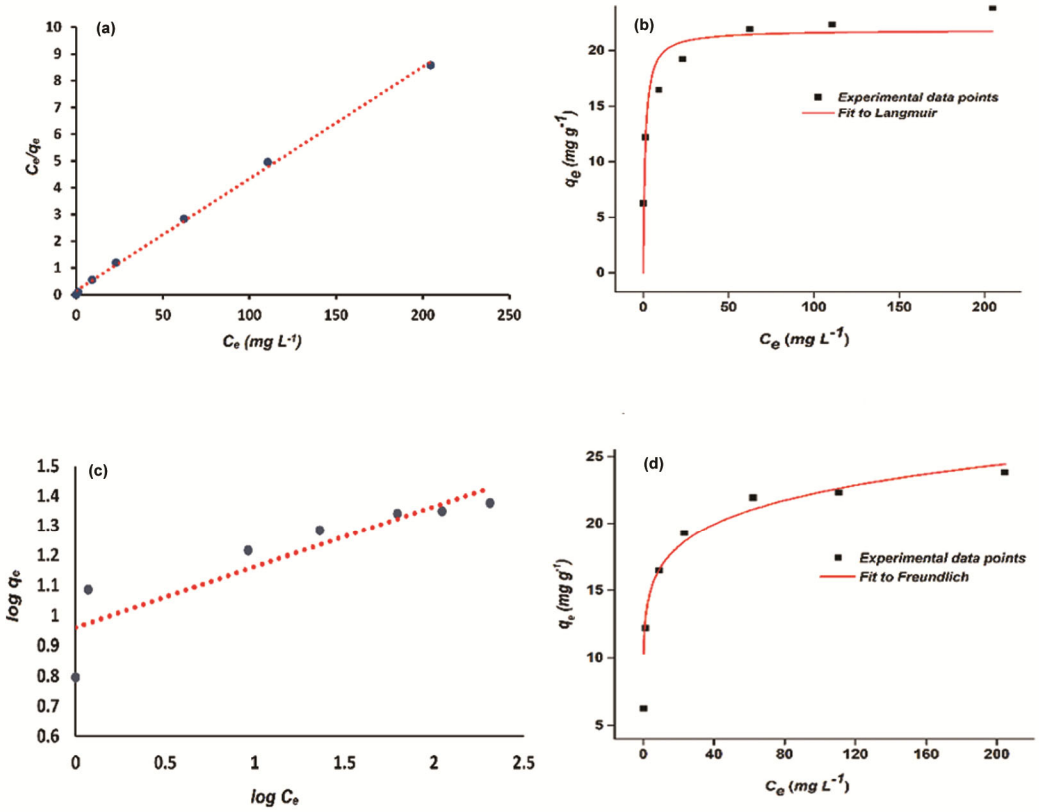

Fig. 4 — (a) Linearized and (b) non- linearized Langmuir isotherm model; (c) linearized and (d) non- linearized Freundlich isotherm model

Table 1 — Isotherm parameters

Isotherm	Parameters	CD sample
Langmuir	q_m (mg g^{-1})	23.88
	K_L	7.036
	R^2	0.998
Freundlich	K_F (mg$^{1-1/n}$/g/L)	0.222
	n	2.797
	R^2	0.910

that controls the process of adsorption[22]. In this study, pseudo-first order[26] and pseudo-second order kinetics[27] model were employed to understand adsorption between solid and liquids. Kinetic study was carried by using 25 mL of 100 mg L^{-1} concentration of Ni (II) solution keeping pH 5.0 with γ-CD dose 100 mg.

The pseudo-first-order kinetics is expressed as follows.

$$\log(q_e - q_t) = \log q_e - (\frac{k_1}{2.303}) \times t \quad \text{... (7)}$$

The nonlinear pseudo-first-order kinetics is expressed as follows.

$$q_t = q_e\,(1 - e^{k_1 * t}) \quad \text{... (8)}$$

Where q_e and q_t denotes the amount of Ni (II) adsorbed in time (t) with first order rate constant denoted by k_1 (min^{-1}). The graph was plotted in between log (q_e-q_t) and time t gives pseudo-first order rate constant with regression coefficient value of 0.838. Linear as well as non-linear plots[28] for pseudo-first-order kinetics was shown in Figs 5 (a) and (b).

The linear equation for pseudo-second order kinetics is expressed as follows.

$$\frac{t}{q_t} = \frac{1}{K_2 \times q_e^2} + \frac{1}{q_e} t \quad \text{.... (9)}$$

The non-linear pseudo-second order kinetics equation is expressed as follows.

$$q_t = \frac{K_2 \times q_e 2 \times t}{1 + K_2 \times q_e \times t} \quad \text{... (10)}$$

Where k_2 is pseudo-second order rate constant expressed in g mg^{-1} min^{-1}. The graph was plotted between log t/q_t and t gives pseudo-second order rate constant.

The value of regression coefficient was found to be

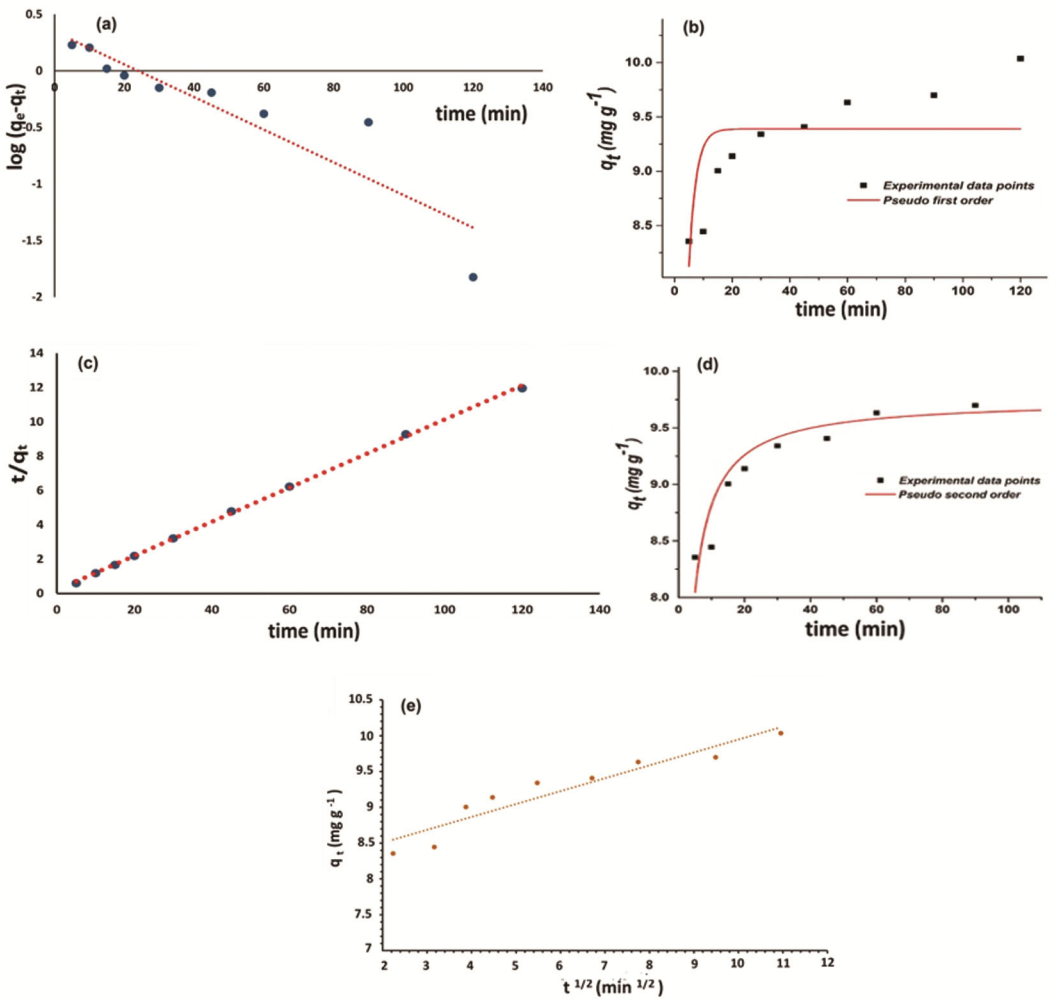

Fig. 5 — Kinetic models of γ-CD: (a) and (b) Linearized and non- linearized plot of pseudo-first order kinetics; (c) and (d) linearized and non- linearized plot of pseudo-second order kinetics; (e) plot for intra-particle diffusion

0.999 for pseudo-second order rate kinetics. Hence pseudo-second order kinetics model was the best fitted model. Figs 5 (c) and (d) show linear and non-linear plots of pseudo-second order kinetics.

In adsorption process, the intraparticle diffusion[29] is rate determining step or not was established by using Weber-Morris equation[30] which is given by the following equation.

$$q_t = k_{int} \times t^{1/2} + C \quad \ldots (11)$$

Graph between q_t and $t^{1/2}$ did not pass through the origin. Hence this indicates that, the diffusion was not a rate limiting step. (Fig. 5e and Table 2). As the value of C is non-zero, it can be predicted that the adsorption process is not only controlled by diffusion.

Thermodynamics of adsorption

Table 2 — Kinetics data

Rate model	Parameters	CD sample
Experimental	q_e	23.88
Pseudo-first order	K_1(min^{-1})	0.033
	R^2	0.838
Pseudo-second order	K_2 (g mg^{-1} min^{-1})	0.007
	R^2	0.999
Intraparticle diffusion	K_{int} (mg g^{-1} min^{-1})	8.146
	R^2	0.897

Thermodynamics establishes spontaneity as well as feasibility of process. To evaluate the Gibb's free energy change at varying temperature ranges van't Hoff plot was studied[31]. Temperature effect on adsorption efficiency was studied by varying temperature from 303, 313, 323 and 333K, with 25 mL of adsorbate solutions with concentration of 100 mg L^{-1} and dose of 100 mg for Ni(II) ions

(Fig. 6). From van't Hoff plot, thermodynamic parameters were calculated (Table 3). The change in the Gibb's free energy[32] (ΔG°) was premeditated by the following equation as-

$$\Delta G^\circ = -RT\ln K \quad ...(12)$$

van't Hoff equation is given by[33]

$$\ln K = \frac{\Delta S^\circ}{R} - \frac{\Delta H^\circ}{RT} \quad ... (13)$$

Exothermic nature of adsorption process[34] is indicated by negative enthalpy change while changes in decrease in arbitrariness of Ni(II) ions is shown by negative entropy change, as it passes from solution to adsorbed state. The adsorption of Ni(II) ions on γ-CD adsorbent was found to be spontaneous with negative Gibb's free energy as shown in Fig. 6. Similar results have been reported for the adsorption of cationic dyes[35,36]. This shows that the adsorption process is completely enthalpy driven in nature[37,38]. The biopolymeric materials generally have found to show similar behaviour as reported in the literature[39].

Table 3 — Thermodynamics of adsorption

ΔG (kJ mol^{-1})				Δ H	Δ S
303 K	313 K	323 K	333 K	(kJ mol^{-1})	(J mol^{-1} K^{-1})
-11.775	-11.574	-10.955	-8.663	-41.567	-96.933

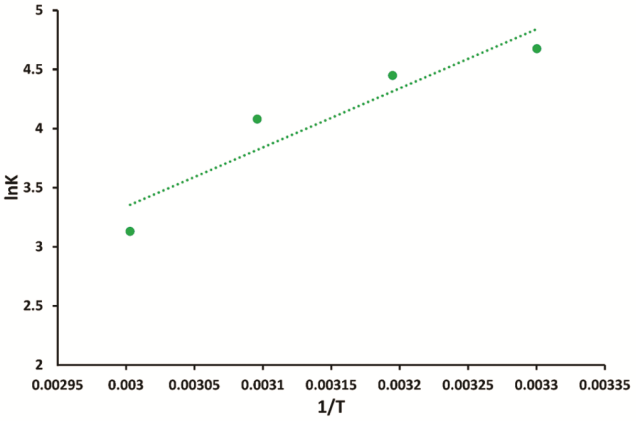

Fig. 6 — van't Hoff plot of γ-CD adsorbent

Column study

Continuous flow analysis thoroughly investigates the concentration difference, leading to a more effective use of the adsorbent potential and enhanced effluent efficiency[35]. For evaluation of dynamic characteristics of fixed-bed column, the shape of the breakthrough curve and the value of breakthrough volume are generally considered as key parameters[40]. In this study, the breakthrough curve is plotted as C_t/C_o versus volume of Ni(II) solution (Fig. 7). This study was conducted by utilizing a glass column having a core diameter of 1 cm and a length of 20 cm. 1 g of γ-CD adsorbent up to a bed height of roughly 10 cm, the column was packed. A known concentration of 100 mg L^{-1} was allowed to percolated through the column. Using a same flow rate of 10 mL min^{-1} as the feed stream, the treated solution was then collected from the bottom of the column and concentration of solution was estimated by using UV-visible spectrophotometer. The column study was repeated until the feed concentration of adsorbate was attained by the concentration of treated solution. As time goes on, these adsorption regions move forward until it reaches the bed exit. In accordance with following equation, breakthrough capacity was calculated[41].

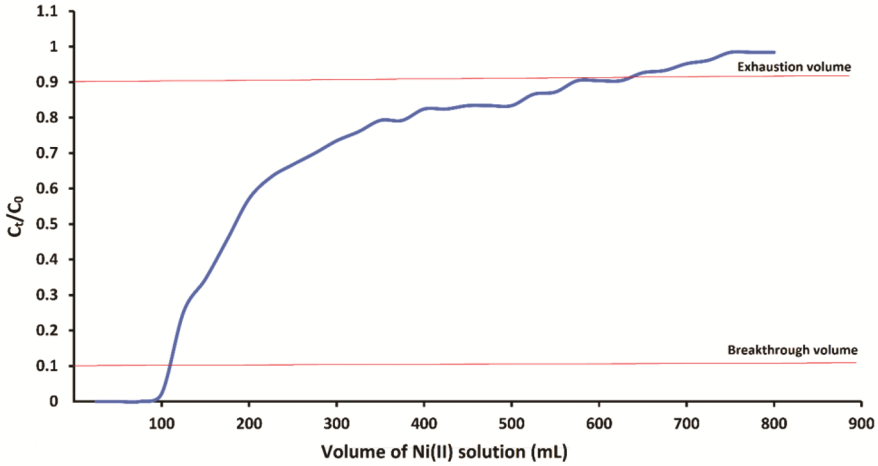

Fig. 7 — Fixed bed column studies using 100 mg L^{-1} Ni(II) concentration with adsorbent dose 100 mg

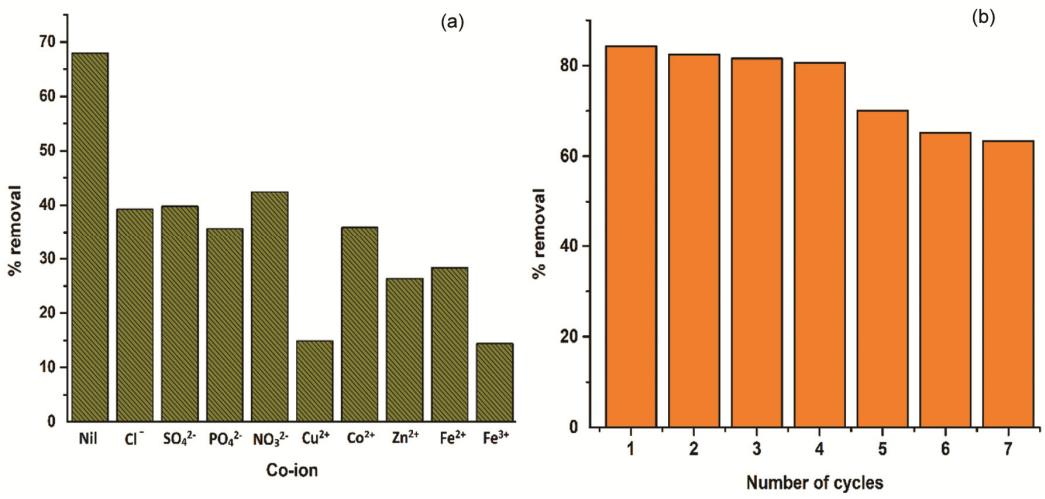

Fig. 8 — (a) Effect of diverse ions on adsorption efficiency and (b) efficiency of regenerated material

$$\text{Exhaustion capacity (mg g}^{-1}) = \frac{\text{exhaustion volume (L)} \times \text{inlet concentration (mg L}^{-1})}{\text{weight of adsorbent (g)}}$$

The exhausted capacity for current work was calculated as 27.5 mg/g for Ni (II). Hence it can be said that, γ-CD can be used as an adsorbent for removal of Ni (II) from water media.

Study of diverse ion

In actual water samples, numerous ions are present which can contest with nickel for the available adsorption sites. To study effect of diverse ions, 100 mg L^{-1} of anions namely chloride, sulphate, nitrate and phosphate as well as cations such as Cu(II), Fe(II), Fe(III), Zn(II) and Co(II) ions were individually selected. 100 mg of adsorbent at pH 5.0, was equilibrated with 100 mg dose and 100 mg L^{-1} solution. It has been observed from Fig. 8a, that phosphate anion and Cu(II) cation affects removal of Ni (II) solution to the greater extent. This can be attributed to higher charge density of phosphate and almost equal ionic radius of copper ions that compete with the nickel ions for the adsorbent surface[42].

Regeneration study and reusability of adsorbent

Material regeneration is very important parameter to study the potent practical application of adsorbent[42]. Reagents used for regeneration are sodium chloride, sodium hydroxide, sodium sulphate and sodium carbonate etc.[43]. From all these reagents, sodium chloride produces best results. For every desorption study, 0.5 M NaCl solution was used. It was found that Ni(II) adsorbed on adsorbent was desorbed very easily. The efficiency of adsorption was reach up to 85% after first cycle and it remains almost constant for next four cycles. As the number of regeneration cycles increases the adsorption efficiency goes on decreases (Fig. 8b).

Table 4 — Comparison of γ-CD with reported literature

Adsorbent	pH	Maximum adsorption efficiency (mg/g)	References
Acid treated Lantana camara fruit	5.0	5.29	44
Waste powdered activated sludge biomass	5.0	13.5	45
H. fusiformis biochar	5.5	12.13	46
Natural sugarcane bagasse	5.0	1.2	47
Brewery sludge	5.0	7.87	48
γ-CD	5.0	23.88	Present study

Comparison with reported literature

Recent literature reports various biomaterials for the removal of Ni(II) ions from water bodies. The main parameter of their relative evaluation is their adsorption capacities. When they are compared on the basis of their efficiencies, it was observed that the γ-CD has better adsorption capacity as compared to most of them. Table 4 is self-explanatory comparison of this material with those reported in literature.

Application to real water samples

The applicability of γ-sterilized biowaste for Ni(II) removal was verified through testing using samples collected from MIDC industrial region of city. 100 mg L^{-1} Ni(II) solution was prepared and spiked into real water samples. γ-sterilized biowaste dose of 100 mg was added into each sample and kept at

Table 5 — Field sample study

Sample name	Initial Ni(II) concentration	Final Ni(II) concentration	Adsorption (%)
MIDC industry	8.31	0.93	89
Siyaram industry	6.22	0.89	86

stirring at room temperature for 60 min. The results obtained have been shown in Table 5 illustrating the adsorption efficiency of γ-sterilized biowaste.

Conclusion

γ-Sterilised cow dung was prepared and successfully used for Ni (II) removal. At pH 5.0, adsorbent dose 100 mg, contact time of 60 min and concentration 100 mg L^{-1} the adsorption capacity was calculated and found to be 23.88 mg/g. The adsorption isotherm was explained best by Langmuir isotherm and equilibrium kinetics was by pseudo second order model. The material was further used for study of diverse ions, regeneration and reusability. It could be concluded that as the adsorbent used is biowaste, the total cost involved in synthesis and pretreatment is completely eliminated. As a result, it is economically viable material. The only limitation is sterilization required before introducing it into water body. This aspect will affect the scaling-up process.

References

1 Jiang J, Shi Y, Ma N L, Ye H, Verma M, Ng H S & Ge S, Utilizing adsorption of wood and its derivatives as an emerging strategy for the treatment of heavy metal-contaminated wastewater, *Environ Pollut*, 340 (2024) 122830.

2 Yang X, Liu L, Wang Y, Lu T, Wang Z & Qiu G, Sustainable and reagent-free cathodic precipitation for high-efficiency removal of heavy metals from soil leachate, *Environ Pollut*, 320 (2023) 121002.

3 Wołowicz A, Staszak K & Hubicki Z, Effect of anionic surfactants on the heavy metal ions removal by adsorption onto ion exchangers-batch and column studies, *J Water Process Eng*, 53 (2023) 103792.

4 Carmona B & Abejón R, Innovative membrane technologies for the treatment of wastewater polluted with heavy metals: Perspective of the potential of electrodialysis, membrane distillation, and forward osmosis from a bibliometric analysis, *Membranes*, 13 (2023) 385.

5 Jima S W, Melesse E Y & Endale A T, Comparison of the removal efficiencies for electro-flotation and electrocoagulation wastewater treatment methods to treat effluents discharged from electroplating industries, *Int J Eng Res Afr*, 63 (2023) 67.

6 Yi J, Wan J, Ye G, Wang Y, Ma Y, Yan Z & Zeng C, Targeted degradation of refractory organic pollutants in wastewater based on molecularly imprinted catalytic materials: Adsorption process and degradation mechanism, *Sep Purif Technol*, 311 (2023) 123244.

7 Aslan S, Yildiz S & Ozturk M, Biosorption of Cu^{2+} and Ni^{2+} ions from aqueous solutions using waste dried activated sludge biomass, *Polish J Chem Technol*, 20 (2018) 20.

8 Rico I L R, Carrazana R J C, Karna N K, Iáñez-Rodríguez I & De Hoces M C, Modeling the mass transfer in biosorption of Cr (VI) y Ni (II) by natural sugarcane bagasse, *Appl Water Sci*, 8 (2018) 55.

9 Kulkarni R M, Vidya S K & Srinikethan G, Kinetic and equilibrium modeling of biosorption of nickel (II) and cadmium (II) on brewery sludge, *Water Sci Technol*, 79 (2019) 888.

10 Chen X, Yu G, Chen Y, Tang S & Su Y, Cow dung-based biochar materials prepared via mixed base and its application in the removal of organic pollutants, *Int J Mol Sci*, 23 (2022) 10094 .

11 Hong S H, Shin M C, Lee J, Lee C G, Song D S, Um B H & Park S J, Recycling of bottom ash derived from combustion of cattle manure and its adsorption behaviors for Cd(II), Cu(II), Pb(II), and Ni(II), *Environ Sci Pollut Res*, 28 (2021) 14957.

12 Singh H & Rattan V K, Adsorption of nickel from aqueous solutions using low cost biowaste adsorbents, *Water Qual Res J*, 46 (2011) 239.

13 Stauber J, Golding L, Peters A, Merrington G, Adams M, Binet M, Batley G, Gissi F, McKnight K, Garman E, Middleton E, Gadd J & Schlekat C, Application of bioavailability models to derive chronic guideline values for nickel in freshwaters of Australia and New Zealand, *Environ Toxicol Chem*, 40 (2021) 100.

14 Wong S, Ngadi N, Inuwa I M & Hassan O, Recent advances in applications of activated carbon from biowaste for wastewater treatment: A short review, *J Clean Prod*, 175 (2018) 361.

15 Iwuozor K O, Emenike E C, Aniagor C O, Iwuchukwu F U, Ibitogbe E M, Okikiola T B, Omuku P E & Adeniyi A G, Removal of pollutants from aqueous media using cow dung-based adsorbents, *Curr Res Green Sust Chem*, 5 (2022) 100300.

16 Wu H, Hanna M A & Jones D D, Thermogravimetric characterization of dairy manure as pyrolysis and combustion feedstocks, *Waste Manage Res*, 30 (2012) 1066.

17 Wan D, Wu L, Liu Y, Zhao H, Fu J & Xiao S, Adsorption of low concentration perchlorate from aqueous solution onto modified cow dung biochar: Effective utilization of cow dung, an agricultural waste, *Sci Total Environ*, 636 (2018) 1396.

18 Saraswat S K, Demir M & Gosu V, Adsorptive removal of heavy metals from industrial effluents using cow dung as the biosorbent: Kinetic and isotherm modeling, *Environ Qual Manage*, 30 (220) (2020) 51.

19 Han X, Zheng Z, Yu C, Deng Y, Ye Q, Niu F, Chen Q, Pan W & Wang Y, Preparation, characterization and antibacterial activity of new ionized chitosan, *Carbohydr Polym*, 290 (2022) 119490.

20 Monteith H D, Shannon E E & Derbyshire J B, The inactivation of a bovine enterovirus and a bovine parvovirus in cattle manure by anaerobic digestion, heat

treatment, gamma irradiation, ensilage and composting, *J Hyg (Lond)*, 97 (1986) 175.
21 Kahu S S, Shekhawat A, Saravanan D & Jugade R M, Two fold modified chitosan for enhanced adsorption of hexavalent chromium from simulated wastewater and industrial effluents, *Carbohydr Polym*, 146 (2016) 264.
22 Doondani P, Jugade R, Gomase V, Shekhawat A, Bampal A & Pandey S, Chitosan/graphite/polyvinyl alcohol magnetic hydrogel microspheres for decontamination of reactive orange 16 dye, *Water J*, 14 (2022) 3411.
23 Khapre M, Shekhawat A, Saravanan D, Pandey S & Jugade R, Mesoporous Fe–Al-doped cellulose for the efficient removal of reactive dyes, *Mater Adv*, 3 (2022) 3278.
24 Rasee A I, Awual E, Rehan A I, Hossain M S, Waliullah R M, Kubra K T, Sheikh M C, Salman M S, Hasan M N, Hasan M M, Marwani H M, Islam A, Khaleque M A & Awual M R, Efficient separation, adsorption, and recovery of Samarium(III) ions using novel ligand-based composite adsorbent, *J Surf Interfac*, 41 (2023) 103276.
25 Khapre M A, Pandey S & Jugade R M, Glutaraldehyde-cross-linked chitosan–alginate composite for organic dyes removal from aqueous solutions, *Int J Biol Macromol*, 190 (2021) 862.
26 Ezzati R, Ezzati S & Azizi M, Exact solution of the Langmuir rate equation: New insights into pseudo-first-order and pseudo-second-order kinetics models for adsorption, *Vacuum*, 220 (2024) 112790.
27 Tran H N, Applying linear forms of pseudo-second-order kinetic model for feasibly identifying errors in the initial periods of time-dependent adsorption datasets, *Water J*, 15 (2023) 1231.
28 Chakraborty V & Das P, Synthesis of nano-silica-coated biochar from thermal conversion of sawdust and its application for Cr removal: Kinetic modelling using linear and nonlinear method and modelling using artificial neural network analysis, *Biomass Conv Bioref*, 13 (2023) 821.
29 Pashchenko D, Intra-particle diffusion limitation for steam methane reforming over a Ni-based catalyst, *Fuel*, 353 (2023) 129205.
30 Bursch M, Mewes J, Hansen A & Grimme S, Best-practice DFT protocols for basic molecular computational chemistry, *Angew Chem Int*, 61 (2022) e202205735.
31 Tandekar S, Korde S & Jugade R M, Red mud-chitosan microspheres for removal of coexistent anions of environmental significance from water bodies, *Carbohydr Polym Technol Appl*, 2 (2021) 100128.
32 Najafi M & Rahimi R, Synthesis of novel Zr-MOF/Cloisite-30B nanocomposite for anionic and cationic dye adsorption: Optimization by design-expert, kinetic, thermodynamic, and adsorption study, *J Inorg Organomet Polym*, 33 (2023) 138.
33 Wang H, Wang S, Wang S, Fu L & Zhang L, The one-step synthesis of a novel metal–organic frameworks for efficient and selective removal of Cr(VI) and Pb(II) from wastewater: Kinetics, thermodynamics and adsorption mechanisms, *J Colloid Interf Sci*, 640 (2023) 230.
34 Darla U R, Lataye D H, Kumar A, Pandit B & Ubaidullah M, Adsorption of phenol using adsorbent derived from saccharum officinarum biomass: Optimization, isotherms, kinetics, and thermodynamic study, *Sci Rep*, 13 (2023) 18356.
35 Bambal A, Jugade R, Khapre M & Saravanan D, Carbonization of golden shower pods to high surface area biochar for decontamination of cationic dyes and regeneration study by gamma radiations, *Next Sustainability*, 5 (2025) 100064.
36 Bambal A, Gomase V, Sarvanan D & Jugade R, Highly efficient mesoporous aluminium-magnetite-alginate magnetic composite for defluoridation of water, *Environ Res*, 261 (2024) 119698.
37 Rathi T, Gomase V & Jugade R M, Torrefaction of cassia fistula seeds for sequestration of aqueous and gaseous pollutants: Experimental and computational approach, *Sustain Chem Environ*, 7 (2024) 100140.
38 Doondhani P, Gomase V & Jugade R M, Novel chitosan-ZnO nanocomposites derived from *Nymphaeaceae fronds* for highly efficient removal of reactive blue 19, reactive orange 16, and congo red dyes, *Environ Res*, 247 (2024) 118228.
39 Gomase V, Doondhani P & Jugade R M, A novel chitosan-barbituric acid hydrogel supersorbent for sequestration of chromium and cyanide ions: Equilibrium studies and optimization through RSM, *Sep Purif Technol*, 330 (2024) 125475.
40 Diniz V & Rath S, Adsorption of aqueous phase contaminants of emerging concern by activated carbon: Comparative fixed-bed column study and in situ regeneration methods, *J Hazard Mater*, 459 (2023) 132197.
41 Safardastgerdi M, Doulati A F & Mahmoodi N M, Lignocellulosic biomass functionalized with EDTA dianhydride for removing Cu (II) and dye from wastewater: Batch and fixed-bed column adsorption, *Miner Eng*, 204 (2023) 108423.
42 Korde S, Tandekar S & Jugade R M, Novel mesoporous chitosan-zirconia-ferrosoferric oxide as magnetic composite for defluoridation of water, *J Environ Chem Eng*, 8 (2020) 104362.
43 Al-dhawi B N S, Optimal parameters for boron recovery in a batch adsorption study: Synthesis, characterization, regeneration, kinetics, and isotherm studies, *Case Studies Chem Environ Eng*, 8 (2023) 100508.
44 Nitya K, Sathish A & Ramchandran T, An insight into the prediction of biosorption mechanism, and isotherm, kinetic and thermodynamic studies for Ni(II) ions removal from aqueous solution using acid treated biosorbent: The Lantana camara fruit, *Desalin Water Treat*, 80 (2017) 276.
45 Aslan S, Yildiz S & Ozturk M, Biosorption of Cu^{2+} and Ni^{2+} ions from aqueous solutions using waste dried activated sludge biomass, *Polish J Chem Technol*, 20 (2018) 20.
46 Shin W, Adsorption characteristics of phenol and heavy metals on biochar from *Hizikia fusiformis*, *Environ Earth Sci*, 76 (2017) 762.
47 Rodríguez R, Carrazana C & Karna K, Modeling the mass transfer in biosorption of Cr (VI) y Ni (II) by natural sugarcane bagasse, *ApplWater Sci,* 8 (2018) 55.
48 Kulkarni R & Srinikethan G, Kinetic and equilibrium modeling of biosorption of nickel (II) and cadmium (II) on brewery sludge, *Water Sci Technol*, 10 (2019) 535472.